Giant drop in the Bardeen-Cooper-Schrieffer coherence length induced by quantum size effects in superconducting nanowires

A. A. Shanenko,[1] M. D. Croitoru,[1,2] A. Vagov,[2] and F. M. Peeters[1]
[1]*Departement Fysica, Universiteit Antwerpen, Groenenborgerlaan 171, B-2020 Antwerpen, Belgium*
[2]*Institute of Theoretical Physics, University of Bayreuth, D-95440 Bayreuth, Germany*
(Received 8 April 2010; revised manuscript received 3 September 2010; published 29 September 2010)

The BCS coherence length in low-dimensional superconductors is dramatically modified by quantum-size effects. In particular, for nanowires made of conventional superconducting materials, we show that the longitudinal zero-temperature coherence length exhibits width-dependent drops by 2–3 orders of magnitude each time when the bottom of one of single-electron subbands formed due to the transverse quantization of electron motion is situated in a close vicinity to the Fermi level. This phenomenon has strong similarities to the well-known BCS-BEC (Bose-Einstein condensation) crossover in ultracold fermionic condensates but with an important exception: it is driven by the transverse quantization of the electron motion rather than by the externally controlled strength of the fermion-fermion interaction.

DOI: 10.1103/PhysRevB.82.104524 PACS number(s): 74.78.Na

I. INTRODUCTION

Superconductors of ultrasmall dimensions possess unusual properties not found in bulk materials. One of them is the quantum-size oscillations, discussed in the pioneering paper by Blatt and Thompson.[1] In quasi-one-dimensional (1D) and -two-dimensional superconducting systems (nanowires and nanofilms) quantization of the transverse electron motion results in single-electron subbands, i.e., in multiple quantum channels for the superconducting condensate. The proximity of the lower edge of such a subband to the Fermi surface leads to a size-dependent enhancement of the superconducting properties, i.e., a superconducting resonance. In particular, such resonances are expected to strongly influence the critical temperature and critical magnetic field (see, e.g., Refs. 1–5). Furthermore, they can result in a remarkable cascade structure of the superconductor-to-normal transition and in the formation of Andreev-type states induced by quantum confinement.[5]

For conventional materials, e.g., Al, Sn, or Pb, the superconducting gap is about 0.1–1.0 meV (Ref. 6) and so, the intersubband energy spacing $\frac{\hbar^2}{2m_e}\frac{\pi^2}{d^2}$ (with d the confining dimension) becomes of the same order or larger for $d \lesssim 20-40$ nm, where quantum-size oscillations of the superconducting properties are expected to be significant. Several recent experimental results on superconducting Pb nanofilms[7,8] and superconducting aluminum/tin nanowires[9] have been attributed to these quantum-size effects (see Refs. 4, 7, and 8, respectively). We remark that superconducting aluminum nanowires with width down to 8–10 nm were recently fabricated.[9,10]

In the present paper we report an unexpected phenomenon due to quantum-size effects, i.e., giant size-dependent variations in the BCS coherence length ξ_0 in low-dimensional superconductors. In all previous theoretical studies of superconducting nanowires and nanofilms, e.g., where phase-slip effects are investigated in nanowires (see, e.g., Ref. 9), one assumes that ξ_0 is given by the same expression as in bulk (the nanowire diameter enters implicitly through the electron mean free path). Contrary to this common assumption, our numerical investigation of the Bogoliubov-de Gennes (BdG) equations[6] for superconducting quantum wires made of conventional materials reveal that, depending on the wire diameter, the zero-temperature longitudinal coherence length varies several orders of magnitude, from values of a few micrometers, typical for conventional bulk superconductors, to a few nanometers, that is usually found in high-T_c materials.[11] This phenomenon has strong similarities to the BCS-BEC crossover in superfluid Fermi gases.[12] However, here this crossover is induced by quantum-size effects rather than by a change in the strength of the fermion-fermion interaction. We remark that the underlying physics of our results is closer to another variant of the BCS-BEC crossover predicted in the pioneering paper by Eagles,[13] i.e., the crossover in superconducting semimetals, where superconducting correlations drive the chemical potential below the bottom of the conduction band. The present consideration is based on the mean-field approximation in the clean limit. However, we show that our main conclusions will not be significantly altered by superconducting fluctuations and imperfections of real metallic nanowires.

The paper is organized as follows. The formalism is outlined in Sec. II. Our main results are discussed in Sec. III. As our consideration is based on the mean-field approach in the clean limit, in Sec. IV we consider issues related to superconducting fluctuations and imperfections of real metallic wires.

II. MODEL AND FORMALISM

We consider a superconducting nanocylinder in the clean limit. For our numerical calculations we take the material parameters of aluminum, the same as in Refs. 4 and 5: $\hbar\omega_D = 32.31$ meV; $gN(0) = 0.18$ [with g the Gor'kov coupling and $N(0)$ the bulk density of states (DOS)]; and $E_F = 0.9$ eV is the effective Fermi level in the parabolic band approximation (for more details, see Ref. 4). Two values for the nanowire diameter are investigated below: $d = 4.22$ nm, for which the nanowire is in the resonance conditions, i.e., the bottom of one of the single-electron subbands is close to the Fermi level and $d = 4.35$ nm, when the nanowire is not

influenced by a superconducting resonance. We note that our conclusions are not sensitive to a particular choice of the parameters as long as $d \lesssim 10-15$ nm; in nanowires of larger diameters quantum-size effects play a less important role.

The internal structure of Cooper pairs is described by $\Psi(\mathbf{x}_1,\mathbf{x}_2)$ (the Cooper-pair wave function) which is related to the anomalous Green's function as

$$\Psi(\mathbf{x}_1,\mathbf{x}_2) = -\lim_{\tau_1-\tau_2\to+0} \mathcal{F}(\mathbf{x}_1\tau_1,\mathbf{x}_2\tau_2), \tag{1}$$

where $\mathcal{F}(\mathbf{x}_1\tau_1,\mathbf{x}_2\tau_2) = -\langle \mathcal{T}\psi_\uparrow(\mathbf{x}_1\tau_1)\psi_\downarrow(\mathbf{x}_2\tau_2)\rangle$ (for the spin-singlet pairing). In what follows we use cylindrical coordinates $\mathbf{x}=(\rho,\varphi,z)$. The diagonal part of Eq. (1), i.e., at $\mathbf{x}_1=\mathbf{x}_2=\mathbf{x}$, is directly related to the superconducting order parameter $\Delta(\mathbf{x}) = g\Psi(\mathbf{x},\mathbf{x})$, where $g>0$ is the Gor'kov coupling constant. Rotational and translational (along the wire) symmetries of the system are reflected in $\Psi(\mathbf{x}_1,\mathbf{x}_2)$ which depends on $\phi=\varphi_1-\varphi_2$ and $z=z_1-z_2$. In turn, the order parameter is a function of ρ only. Here, we are interested in the structure of a Cooper pair *along* the wire and, therefore, consider the quantity

$$\Psi(\rho,z) = \Psi(\rho,\varphi,z_1+z;\rho,\varphi,z_1). \tag{2}$$

The anomalous Green's function can be expressed in terms of the eigenstates of the BdG equations (see, e.g., Ref. 6) which, following the system symmetry, are specified by the radial quantum number j, azimuthal quantum number m, and wave vector k of the quasifree particle motion along the wire. This defines 1D subbands labeled by (j,m). For $T=0$ the wave function in Eq. (2) can be written as a sum over such subbands as

$$\Psi(\rho,z) = \sum_{jm} \Psi_{jm}(\rho,z) \tag{3}$$

with the subband contribution given by

$$\Psi_{jm}(\rho,z) = \frac{1}{(2\pi)^2}\int dk u_{jmk}(\rho)v^*_{jmk}(\rho)e^{\imath kz}. \tag{4}$$

Here $u_{jmk}(\rho)$ and $v_{jmk}(\rho)$ obey the BdG equations written as

$$E_{jmk}\begin{pmatrix} u_{jmk} \\ v_{jmk}\end{pmatrix} = \begin{pmatrix} \hat{H}_{mk} & \Delta(\rho) \\ \Delta^*(\rho) & -\hat{H}^*_{mk}\end{pmatrix}\begin{pmatrix} u_{jmk} \\ v_{jmk}\end{pmatrix} \tag{5}$$

with E_{jmk} the quasiparticle energy and

$$\hat{H}_{mk} = -\frac{\hbar^2}{2m_e}\left[\frac{1}{\rho}\frac{\partial}{\partial\rho}\rho\frac{\partial}{\partial\rho} - \frac{m^2}{\rho^2} - k^2\right] - E_F,$$

where m_e is the electron band mass taken equal to the free-electron mass. Solutions of Eq. (5) are set to zero at the wire boundary (quantum confinement).

III. BCS COHERENCE LENGTH DRIVEN BY QUANTUM-SIZE EFFECTS

A. Qualitative picture

The integral over k in Eq. (4) is restricted to the Debye window, i.e., $|\zeta_{jmk}|<\hbar\omega_D$ with ζ_{jmk} the subband single-particle dispersion $\zeta_{jmk}=\hbar^2k^2/2m_e-\mu_{jm}$, where $\mu_{jm}=E_F-\varepsilon_{jm}$ is the chemical potential measured from the subband lower edge (bottom) energy ε_{jm}. Note that μ_{jm} controls the longitudinal momentum distribution and, so, plays the role of the subband-dependent "longitudinal chemical potential." Figure 1(a) shows a sketch of the single-particle energies for the subbands with $j=0$ and $m=0,\pm1,\pm2$. The dotted horizontal lines in Fig. 1(a) highlight the Debye window that determines the upper k^+_{jm} and lower k^-_{jm} limits for k in the integral in Eq. (4).

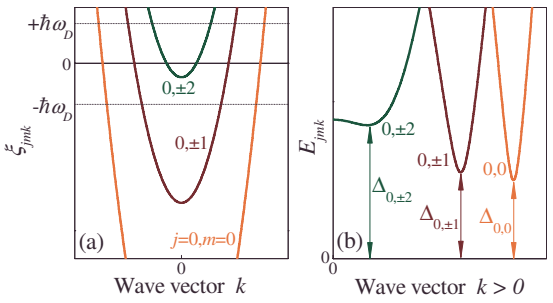

FIG. 1. (Color online) (a) Single-electron energies ζ_{jmk} (measured from the Fermi level E_F) versus the wave vector for the longitudinal motion k in subbands $(j,m)=(0,0)$, $(0,\pm1)$, and $(0,\pm2)$. Horizontal dotted lines denote the Debye window. (b) Quasiparticle energies E_{jmk} as function of k for the same subbands.

The bottoms of all single-electron subbands shift in energy with changing diameter. A quantum-size superconducting resonance develops when the bottom of a subband comes into the Debye window, i.e., when $|\mu_{jm}|<\hbar\omega_D$. In Fig. 1(a) subbands $(0,\pm2)$ satisfy this condition. Below they are referred to as resonant subbands. Any subband generates a quantum channel for the formation of the superconducting condensate. In a simplified picture one can utilize Anderson's approximate solution of the BdG equations (see, e.g., Ref. 5), which assumes that the spatial dependence of both $u_{jmk}(\rho)$ and $v_{jmk}(\rho)$ is given by the radial single-electron wave function $\vartheta_{jm}(\rho)$ (proportional to the Bessel function of the first kind). This leads to $E_{jmk}=\sqrt{\zeta^2_{jmk}+\Delta^2_{jm}}$ with Δ_{jm} the subband energy gap as schematically shown in Fig. 1(b).

Within Anderson's approximation, Eq. (4) reduces to

$$\Psi_{jm}(\rho,z) = \frac{\vartheta^2_{jm}(\rho)}{(2\pi)^2}\int_{k^-_{jm}}^{k^+_{jm}} dk\frac{\Delta_{jm}\cos(kz)}{\sqrt{\zeta^2_{jmk}+\Delta^2_{jm}}}. \tag{6}$$

When $\Delta_{jm}\ll\hbar\omega_D$, the upper limit in the integral can be extended to infinity while the lower one can be set to zero (for negative μ_{jm} we also need $|\mu_{jm}|\ll\hbar\omega_D$). This yields an exponentially decaying function of z, and its decay length defines the subband (channel) BCS coherence length $\xi_0^{(jm)}$. For its analytical estimate, we use the contour integration in the complex plane. The integrand in Eq. (6) has four singular points (the square-root branch points) with the same absolute value of the imaginary part, i.e., $[m_e(\sqrt{\mu^2_{jm}+\Delta^2_{jm}}-\mu_{jm})]^{1/2}/\hbar$. For, say, positive z, the contour is closed in the upper half plane and distorted to encircle the cut between the two upper singular points. Their imaginary part controls $\xi_0^{(jm)}$, i.e.,

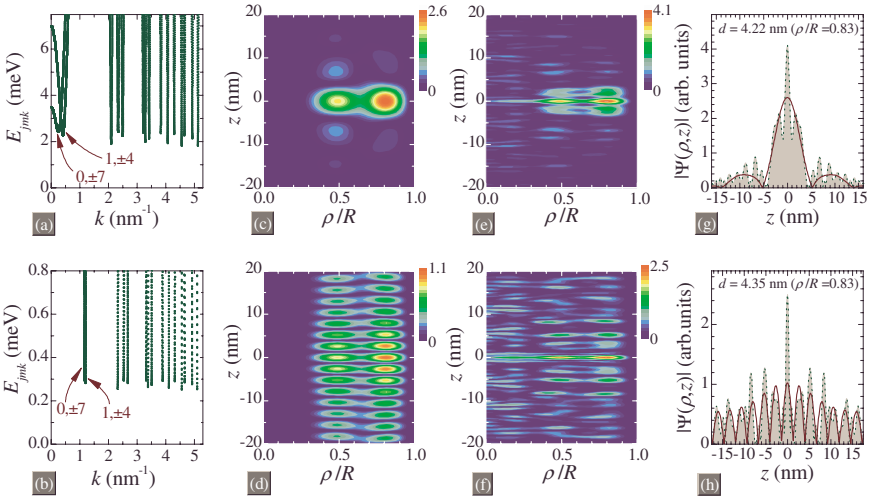

FIG. 2. (Color online) The resonant wire, d=4.22 nm: (a) the quasiparticle-energy dispersion E_{jmk}, the resonant subbands are $(j,m)=(0,\pm 7)$ and $(1,\pm 4)$; (c) the contour plot of $|\Psi(\rho,z)|$ (arbitrary units) when accounting only for subbands $(0,\pm 7)$ and $(1,\pm 4)$; (e) the same but for the total Cooper-pair wave function; (g) the longitudinal profile of $|\Psi(\rho,z)|$ at ρ/R=0.83 with all relevant quantum channels included (dotted curve) and when only contributions of $(0,\pm 7)$ and $(1,\pm 4)$ are taken (solid curve). Panels (b), (d), (f), and (h) display the same but for the nonresonant wire at d=4.35 nm.

$$\xi_0^{(jm)} = \frac{\hbar}{\sqrt{m_e}}[\sqrt{\mu_{jm}^2+\Delta_{jm}^2}-\mu_{jm}]^{-1/2}. \quad (7)$$

As seen from Eq. (7), $\xi_0^{(jm)}$ decreases when μ_{jm} goes from positive to negative values. When $\mu_{jm}/\Delta_{jm} \gg 1$ we have the conventional result for the BCS coherence length, i.e., $\xi_0^{(jm)} \approx \hbar v_{jm}/\Delta_{jm}$ with $v_{jm}=\sqrt{2\mu_{jm}/m_e}$ the subband Fermi wave vector. At resonance, i.e., for $\mu_{jm}\to 0$, we find from Eq. (7) a very different expression $\xi_0^{(jm)} \approx \hbar/(m_e\Delta_{jm})^{1/2}$. Finally, for $\mu_{jm}<0$ and $|\mu_{jm}| \gg \Delta_{jm}$, we obtain $\xi_0^{(jm)} \approx \hbar/(2m_e|\mu_{jm}|)^{1/2}$, which decreases with increasing $|\mu_{jm}|$. Thus, we have a drop in the BCS coherence length of the resonant subband(s) and, at the same time, such a subband(s) provides a major contribution to Eq. (3) due to a significantly enhanced DOS in the Debye window.

We note that for $\mu_{jm}<0$, Eq. (7) becomes similar to the expression for the fermion-pair size at the BEC side of the BCS-BEC crossover in superfluid Fermi gases [see discussion after Eq. (140) in Ref. 12], where the chemical potential μ and the order parameter Δ should be replaced by μ_{jm} and Δ_{jm}, respectively. Hence, following the asymptotic $\xi_0^{(jm)} \propto |\mu_{jm}|^{-1/2}$ (for $\mu_{jm}<0$), we can interpret $|\mu_{jm}|$ as the pair binding energy in the corresponding quantum channel. One can see that the Cooper pairs are much stronger confined when μ_{jm} becomes negative, in an apparent similarity with the BCS-BEC crossover. However, μ_{jm} becomes negative due to quantum-size effects instead of a change in the strength of the pair interaction. Another difference is that the contribution of a subband to the pair condensate is strongly reduced when $|\mu_{jm}|$ approaches $\hbar\omega_D$ and disappears completely for $\mu_{jm}<-\hbar\omega_D$.

B. Numerical solution

A numerical self-consistent solution of the BdG Eq. (5) gives the results shown in Figs. 2 and 3. In Fig. 2(a) E_{jmk} is given versus k for d=4.22 nm. Here the bottoms of the two subbands with $(j,m)=(0,\pm 7)$ and $(1,\pm 4)$ are in the Debye window and, so, $v_{0,\pm 7}$ and $v_{1,\pm 4}$ (recall that $v_{jm}=\sqrt{2\mu_{jm}/m_e}$) are extremely small. E_{jmk} for the nonresonant wire with d =4.35 nm is shown in Fig. 2(b). Here the corresponding single-electron spectrum has no resonant subbands and $v_{0,\pm 7}$ and $v_{1,\pm 4}$ are larger by an order of magnitude as compared to panel (a). Numerical results for the resonant case exhibit a significant increase in $\Delta_{0,\pm 7}$ and $\Delta_{1,\pm 4}$ and, in turn, lead to enhanced superconducting gaps in the other quantum channels. When the resonance decays (i.e., due to a change in d), all Δ_{jm} are reduced and approach the bulk value Δ_{bulk} =0.25 meV.

The contour plots in Figs. 2(c) and 2(d), for the resonant and nonresonant wires, respectively, display the absolute value of $\Psi(\rho,z)$, as calculated from Eq. (3) but with the summation restricted to subbands $(0,\pm 7)$ and $(1,\pm 4)$. Panels (e) (for d=4.22 nm) and (f) (for d=4.35 nm) show the total quantity $|\Psi(\rho,z)|$, where we summed over all relevant subbands. For the resonant case, illustrated by panels (c) and

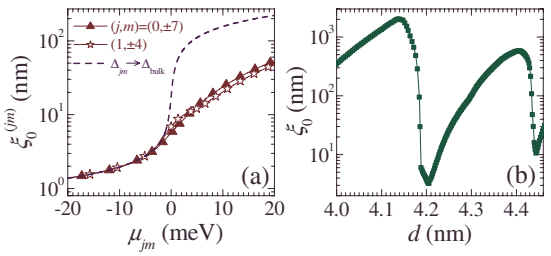

FIG. 3. (Color online) BCS-BEC crossover induced by quantum-size effects: (a) the subband longitudinal BCS coherence length $\xi_0^{(jm)}$ versus μ_{jm} as numerically calculated from the BdG equations for $(j,m)=(0,\pm 7)$ (triangles) and $(1,\pm 4)$ (stars), the dashed curve represents Eq. (7) with Δ_{jm} replaced by Δ_{bulk}; (b) the total longitudinal BCS coherence length ξ_0 versus the nanowire diameter.

(e), the longitudinal distribution of electrons is well localized whereas an oscillating and weakly decaying dependence appear in panels (d) and (f). This is also clearly seen from panels (g) and (h) representing the longitudinal profile of $|\Psi(\rho,z)|$ at $\rho/R=0.83$ [i.e., the maximum point of $\Psi(\rho,z=0)$] for the resonant and nonresonant wires, respectively. Here the dotted curve gives the total contribution of all subbands whereas the solid line corresponds to a contribution from only $(j,m)=(0,\pm 7)$ and $(1,\pm 4)$. Thus, the resonant subbands control $\Psi(\rho,z)$, and the corresponding longitudinal distribution of electrons in a Cooper pair is strongly localized. At $d=4.35$ nm single-electron subbands $(j,m)=(0,\pm 7)$ and $(1,\pm 4)$ are shifted down as compared to their positions at $d=4.22$ nm. As a result, the resonance disappears and the relative contribution of the states with $(j,m)=(0,\pm 7)$ and $(1,\pm 4)$ to the superconducting order parameter $\Delta(\rho)=\Psi(\rho,z=0)$ drops to 40%, see panel (h). Nevertheless, the longitudinal decay of $\Psi(\rho,z)$ is still mainly determined by these states.

The longitudinal BCS coherence length ξ_0 is defined as the decay length of $\Psi(\rho,z)$ in the z direction and can be calculated through a numerical fit. For both the partial and total wave functions, such a fitting gives similar values: ~ 1 μm for the nonresonant wire and ≈ 5 nm for the resonant case. The latter value is almost three orders of magnitude less than the BCS coherence length in bulk aluminum (≈ 1.6 μm) and is comparable to the one in high-T_c superconductors.[11] Further insight can be obtained from Figs. 3(a) and 3(b). Panel (a) demonstrates numerical results for $\xi_0^{(jm)}$ as function of μ_{jm} for $(j,m)=(0,\pm 7)$ (triangles) and $(1,\pm 4)$ (stars). Notice that these data are in good agreement with the analytical formula of Eq. (7). When substituting Δ_{bulk} for Δ_{jm} in Eq. (7), we obtain the dashed curve approaching our numerical results for $\mu_{jm}<0$. In this case $\xi_0^{(jm)}\approx\hbar/(2m_e|\mu_{jm}|)^{1/2}$ is not sensitive any more to Δ_{jm}. Finally, Fig. 3(b) illustrates how the total longitudinal BCS coherence length ξ_0 depends on d. Its value is minimal at $d=4.22$ nm, and the difference between the maximum and minimum is roughly 2–3 orders of magnitude. As seen from Fig. 3(b), the next superconducting resonance comes into play at $d=4.44$ nm. Our illustrative choice of nanowires with $d\sim 4$ nm is not crucial and given for simplicity: it is easier to explain the underlying physics in the presence of a small number of relevant single-electron subbands, i.e., for smaller diameters. When increasing d, quantum-size-driven drops of ξ_0 are weakened but still pronounced up to diameters of about 10 nm. The effect of interest is washed out only when $d\gtrsim 20$ nm.

IV. DISCUSSION

A. Effects of the surface roughness

Our previous consideration was limited to the clean limit and assumed specular reflections of electron waves from the nanowire boundaries. To what extent imperfections of real metallic nanowires can influence our predictions? In recently fabricated high-quality superconducting nanowires the superconducting state survives down to diameters of about 8–10 nm without signatures of suppression of T_c by disorder. Unlike strongly disordered nanoscale superconductors, such high-quality superconducting nanowires exhibit a systematic shift-up of the critical temperature with a reduction in their cross section. This shift is about 50% (as compared to bulk) in Al nanowires[9,10,14] with diameters of about 8–10 nm and 10–20 % in Sn specimens[15–17] with width down to 15–20 nm. As recently shown (see the first paper in Ref. 4), it is the quantization of the transverse electron motion that shifts T_c up in such nanowires through the formation of quantum-size superconducting resonances. Thus, we can expect that disorder is relatively minor in high-quality superconducting nanowires and, so, scattering on imperfections does not shadow the appearance of well-distinguished single-electron subbands that form due to the transverse quantum confinement.

To go in more detail, surface roughness is a major disorder mechanism in high-quality superconducting nanowires. Indeed, in most papers[9,10,14] the mean free path was estimated to approximately follow the nanowire width $\ell\sim d$, i.e., elastic scattering on the boundary imperfections controls the electron mean free path. It is instructive to compare the longitudinal BCS coherence length ξ_0 calculated in Sec. III with the electron mean free path. When approaching a quantum-size superconducting resonance, ξ_0 drops down to values close to the nanowire diameter, see, e.g., Fig. 3 (this is true for nanowires with $d<10-20$ nm, for larger diameters the effect is washed out). As the mean free electron path ℓ follows d, we obtain $\xi_0\approx\ell$. This means that elastic scattering on surface imperfections cannot significantly alter our conclusions about the size-dependent drops of ξ_0.

The above reasoning assumes that the density of single-electron states at the Fermi level does not change significantly in the presence of surface imperfections. So, we also need to clarify if the single-electron spectrum can be significantly influenced by surface roughness. As discussed in Sec. III, a pronounced size-dependent drop of ξ_0 occurs each time when the bottom of a single-electron subband crosses the Fermi level. The longitudinal motion of electrons in such a subband is significantly suppressed, which results in long longitudinal electron wavelengths. Typical longitudinal electron energies in a resonant subband are about or less than the Debye energy $\hbar\omega_D$ and, so, the corresponding longitudinal wavelengths of electrons are governed by the scale $2\pi\sqrt{\frac{\hbar}{m_e\omega_D}}\sim 10$ nm. This is significantly larger than the characteristic size of the surface imperfections (it is about or smaller than 1–2 nm in nanowires with diameters less than 10 nm, see the next paragraph). Hence, the longitudinal motion of electrons in a resonant subband appears to be quite stable against surface imperfections. This is, of course, not the case for subbands with bottoms far below the Fermi surface. However, such subbands make a minor contribution at superconducting resonances.

In addition to the influence of surface roughness on the longitudinal electron motion, one should also take into account fluctuations of the transverse electron energy resulting from fluctuations in the nanowire diameter. When approaching the Debye-energy scale, such fluctuations of the subband bottoms can smooth superconducting resonances. However, a simple estimate shows that this can be expected for ultranarrow nanowires with diameters less than 2–3 nm. As already mentioned in the Sec. I, the energy spacing between

the single-electron subbands is about $\frac{\hbar^2}{2m_e}\frac{\pi^2}{d^2}$. When assuming $d=\bar{d}+\delta d$, where δd represents the fluctuating contribution and $\bar{d}$ stands for the average diameter, the uncertainty in the intersubband spacing due to δd is given by $\frac{\hbar^2}{m_e}\frac{\pi^2}{\bar{d}^3}\delta d$. Let us set $|\delta d| \sim 0.1\bar{d}-0.2\bar{d}$ (see, for instance, experimental results from Ref. 14). Then, we obtain $\frac{\hbar^2}{m_e}\frac{\pi^2}{\bar{d}^3}\delta d > \hbar\omega_D$ for $d < 2-3$ nm. For $d=4-5$ nm the above uncertainty is about few millielectron volt, which is much smaller than $\hbar\omega_D = 32.1$ meV (for aluminum). So, even for very small diameters about 4 nm chosen for a simple illustration in Figs. 2 and 3 (to avoid a discussion of many single-particle subbands) fluctuations of the transverse electron levels has no significant effect on the formation of the resonances.

Another possible reason for broadening of the single-electron levels is the hybridization with electrons of a semiconductor substrate, which depends strongly on the fabrication conditions. However, such a hybridization can be expected to be of importance for specimens with width down to a few monolayers like in ultrathin superconducting nanofilms.

Thus, based on the above discussion, we can conclude that our results are not very sensitive to imperfections in real superconducting nanowires, i.e., surface roughness and nonuniform cross section. These imperfections can smooth the quantum-size oscillations in ξ_0 (see, e.g., our remark in Ref. 18) but will not cancel the effect.

B. Fluctuations

Our investigation is based on the mean-field approximation and, so, one more point to discuss is fluctuations of the superconducting condensate. It is well known that fluctuations generally play a more important role in low-dimensional systems. In superconducting nanowires the main focus is usually on phase fluctuations of the pair condensate: thermally activated and quantum phase slips, see, e.g., Ref. 9. These fluctuations lead to a residual resistance remaining below T_c in narrow nanowires and, so, corrupting the superconducting state.

Effect of thermal fluctuations is usually estimated with the Ginzburg-Levanyuk parameter Gi calculated from the conventional Ginzburg-Landau functional (see, e.g., textbooks[19,20] and original papers[21,22]). When assuming that the order parameter is position independent in the direction perpendicular to the nanowire (quasi-1D version of the Ginzburg-Landau formalism), one can obtain

$$Gi = \left[\frac{7\zeta(3)T_F}{2^{3/2}\pi T_c(k_F d)^2 k_F \xi_0}\right]^{2/3} \approx \left[\frac{T_F}{T_c(k_F d)^2 k_F \xi_0}\right]^{2/3}, \quad (8)$$

where T_F is the Fermi temperature and $\zeta(3)\approx 1.2$ (for basic formulas, see, e.g., textbook[20] reproducing calculations dating back to Levanyuk's paper[21]). Typical resonant enhancements of T_c in the vicinity of, say, $d\approx 10$ nm are $k_B T_c \approx 0.3-0.5$ meV (this is 1.5–2 times the bulk critical temperature for our parameters, see the first paper in Ref. 4). So, assuming that ξ_0 drops down to $\approx d$, one can find from Eq. (8) that $Gi\approx 0.1$, which means that thermal fluctuations are of importance for temperatures $T/T_c > 1-Gi=0.9$. For nonresonant diameters situated in the same domain around $d=10$ nm the Ginzburg-Levanyuk parameter is by an order of magnitude smaller, i.e., $Gi\approx 0.01$ (here T_c and ξ_0 are approximately the same as in bulk). Equation (8) means that as the nanowire diameter decreases, the Ginzburg-Levanyuk parameter increases: impact of fluctuations is enhanced, as expected. However, even for resonances located in the vicinity of $d=4-5$ nm we have $Gi\approx 0.2$ [here the typical resonant enhancements of the critical temperature are on the scale of $k_B T_c = 1.1-1.4$ meV, as seen from the excitation spectrum in Fig. 1(a)]. Here it is worth noting that Eq. (8) can give us only a qualitative trend because, strictly speaking, the conventional Ginzburg-Landau formalism is not well justified for superconducting specimens with dimensions smaller than the zero-temperature bulk coherence length (on the order of microns for weak-coupling superconductors, e.g., aluminum). In particular, the translational invariance in the direction perpendicular to the nanowire is broken due to quantum confinement. As a consequence, the order parameter can strongly vary with the transverse coordinates (see, e.g., Refs. 4 and 23), and the scale of its variations ($\sim d$) is the same as that of the integral kernels in the nonlinear integral equation for the order parameter resulting from the expansion of the self-consistency equation in powers of $\Delta(\mathbf{x})$. This may question the use of the local approximation in order to reduce the above integral equation to the conventional Ginzburg-Landau equation having the simpler differential structure (see details of the Gor'kov derivation in, e.g., textbook[24]).

As is well known, temperatures far below T_c are the domain of quantum fluctuations. In particular, as seen from the results reported in papers,[10,14] quantum phase slips in aluminum superconducting nanowires with diameters about 10 nm produce a residual resistance even at temperatures below $0.6T_c$. For these diameters such a residual resistance is almost insignificant, i.e., it is on the order of 10^{-5} in units of the normal resistance. However, it is expected that for smaller diameters quantum-phase slips will proliferate, resulting in a superconductor-to-normal crossover at $d=d_c$ with $d_c \lesssim 10$ nm (see, e.g., Ref. 9). Recent results of Ref. 14 suggest that this kind of dissipative phase transition occurs when the nanowire diameter approaches 8 nm, i.e., $d_c \approx 8$ nm. Yet, it is rather difficult to analyze experimental data for very narrow nanowires because it is not possible to completely rule out weak links as the sources of the residual resistance.[25]

Thus, the mean-field treatment appears to be quite justified for nanowires with diameters larger than $d_c \approx 8$ nm. We remark that drops of ξ_0 driven by quantum-size effects are expected to be pronounced for $d<10$ nm and washed out only when $d>20$ nm. In addition, our results can be of relevance for $d<d_c$, because the mean-field coherence length is an important parameter controlling the rate of quantum-phase slips and, so, the residual resistance significantly below T_c.[9,26] Here it is worth noting that a simple estimate shows that the pronounced size-dependent drops of the coherence length ξ ($\xi\to\xi_0$ when $T\to 0$) have a significant effect on the residual resistance $R_{\rm res}$ of superconducting nanowires. In particular, when assuming that the normal-state resistance of the nanowire R_N is close to the resistance quan-

tum given by $R_Q = \pi \frac{\hbar^2}{2e^2}$ (this is true for narrow enough nanowires), one can obtain[9,14,26]

$$\frac{R_{\rm res}}{R_N} \sim \frac{L}{\xi} e^{-L/\xi},$$

where L stands for the nanowire width. The above relation shows that $R_{\rm res}/R_N$ significantly falls down at the quantum-size driven drops of the coherence length. This can open interesting prospects of observing quantum-size effects in the residual resistance of superconducting nanowires.

V. CONCLUSION

In conclusion, we have demonstrated that the longitudinal BCS coherence length of a superconducting metallic nanowire undergoes width-dependent giant drops of several orders of magnitude. This occurs each time when a transverse discrete single-electron level is positioned in the vicinity of the Fermi surface so that the longitudinal motion in the corresponding single-electron subband (making a major contribution to the superconducting characteristics) is significantly suppressed. This behavior of ξ_0 provides a substantial insight on the underlying physics of superconducting quantum-size oscillations: the phenomenon appears to be similar to the BCS-BEC crossover in superfluid Fermi gases. However, there is an important exception: it is driven by the transverse quantization of the electron motion rather than by the externally controlled strength of the fermion-fermion interaction. One can expect that the size-dependent drops of the zero-temperature coherence length is a generic feature of low-dimensional superconducting structures where the pair condensate is facilitated via multiple channels (subbands), e.g., superconducting nanofilms. However, in the presence of imperfections of real samples, quantum-size-driven drops of the coherence length can be smoothed in an overall decrease in ξ_0 with decreasing the quantum-confined dimensions. We note that, apart from setting the system close to or far from the superconducting resonance, a particular choice of the parameters is not important for the main conclusions. Also we note that the sharp Debye window boundaries for the pairing are not necessary for the validity of the conclusions, and our results are not sensitive to the cut-off regularization of the BCS approach.

ACKNOWLEDGMENTS

This work was supported by the Flemish Science Foundation (FWO-Vl), the Belgian Science Policy (IAP), and the ESF-network: INSTANS. M.D.C. acknowledges support from the Alexander von Humboldt Foundation. A.A.S. thanks R. G. Mints, W. V. Pogosov, D. Y. Vodolazov, A. Perali, and A. Bianconi for fruitful discussions.

[1] J. M. Blatt and C. J. Thompson, Phys. Rev. Lett. **10**, 332 (1963).
[2] M. Strongin, R. S. Thompson, O. F. Kammerer, and J. E. Crow, Phys. Rev. B **1**, 1078 (1970).
[3] A. Perali, A. Bianconi, A. Lanzara, and N. L. Saini, Solid State Commun. **100**, 181 (1996).
[4] A. A. Shanenko, M. D. Croitoru, M. Zgirski, F. M. Peeters, and K. Arutyunov, Phys. Rev. B **74**, 052502 (2006); A. A. Shanenko, M. D. Croitoru, and F. M. Peeters, *ibid.* **75**, 014519 (2007).
[5] A. A. Shanenko, M. D. Croitoru, and F. M. Peeters, Phys. Rev. B **78**, 054505 (2008); A. A. Shanenko, M. D. Croitoru, R. G. Mints, and F. M. Peeters, Phys. Rev. Lett. **99**, 067007 (2007).
[6] P. G. de Gennes, *Superconductivity of Metals and Alloys* (W. A. Bejamin, New York, 1966).
[7] Y. Guo, Y.-F. Zhang, X.-Y. Bao, T.-Z. Han, Z. Tang, L.-X. Zhang, W.-G. Zhu, E. G. Wang, Q. Niu, Z. Q. Qiu, J.-F. Jia, Z.-X. Zhao, and Q.-K. Xue, Science **306**, 1915 (2004).
[8] D. Eom, S. Qin, M.-Y. Chou, and C. K. Shih, Phys. Rev. Lett. **96**, 027005 (2006).
[9] K. Yu. Arutyunov, D. S. Golubev, and A. D. Zaikin, Phys. Rep. **464**, 1 (2008).
[10] F. Altomare, A. M. Chang, M. R. Melloch, Y. Hong, and C. W. Tu, Phys. Rev. Lett. **97**, 017001 (2006).
[11] G. Deutscher, *New Superconductors: From Granular to High T_c* (World Scientific, Singapore, 2006).
[12] I. Bloch, J. Dalibard, and W. Zwerger, Rev. Mod. Phys. **80**, 885 (2008).
[13] D. M. Eagles, Phys. Rev. **186**, 456 (1969).
[14] M. Zgirski, K.-P. Riikonen, V. Touboltsev, and K. Arutyunov, Nano Lett. **5**, 1029 (2005).
[15] M. L. Tian, J. G. Wang, J. S. Kurtz, Y. Liu, M. H. W. Chan, T. S. Mayer, and T. E. Mallouk, Phys. Rev. B **71**, 104521 (2005).
[16] L. Jankovič, D. Gournis, P. N. Trikalitis, I. Arfaoui, T. Cren, P. Rudolf, M. H. Sage, T. T. M. Palstra, B. Kooi, J. De Hosson, M. A. Karakassides, K. Dimos, A. Moukarika, and T. Bakas, Nano Lett. **6**, 1131 (2006).
[17] N. Tombros, L. Buit, I. Arfaoui, T. Tsoufis, D. Gournis, P. N. Trikalitis, S. J. van der Molen, P. Rudolf, and B. J. van Wees, Nano Lett. **8**, 3060 (2008).
[18] This is similar to the quantum-size oscillations of the critical temperature reported in our previous papers (see, e.g., Ref. 4): width-dependent oscillations of the critical temperature accompanied by pronounced size-dependent resonant enhancements are smoothed in real nanowires into an overall enhancement with decreasing nanowire cross section.
[19] A. Z. Patashinskii and V. L. Pokrovskii, *Fluctuation Theory of Phase Transitions* (Pergamon, Oxford, 1979).
[20] J. B. Ketterson and S. N. Song, *Superconductivity* (Cambridge University Press, Cambridge, 1999).
[21] A. P. Levanyuk, Sov. Phys. JETP **36**, 571 (1959).
[22] V. L. Ginzburg, Sov. Phys. Solid State **2**, 1824 (1960).
[23] I. Grigorenko, J. X. Zhu, and A. Balatsky, J. Phys.: Condens. Matter **20**, 195204 (2008).
[24] A. L. Fetter and J. D. Walecka, *Quantum Theory of Many-Particle Systems* (Dover, Mineola, 2003).
[25] M. Zgirski and K. Yu. Arutyunov, Phys. Rev. B **75**, 172509 (2007).
[26] D. S. Golubev and A. D. Zaikin, Phys. Rev. B **64**, 014504 (2001).